Bluebild: A Next-Generation Radio Interferometric Imager

Sepand Kashani, Matthieu Simeoni, Paul Hurley, Jean-Paul Kneib, Emma Tolley, Simon Frasch, Etienne Orliac, Michele Bianco, Arpan Das, Shreyam Parth Krishna

SKACH Winter Meeting 2023, Zurich, Switzerland - 22/01/2024

Next-Generation Radio Interferometry Team

- Leading PASC proposal to optimize, validate, and integrate Bluebild in precursor pipelines
- Team:
  - **Emma Tolley**: Team leader
  - **Etienne Orliac**: HPC expert @ EPFL working on benchmarking, optimization, C & CUDA kernels
  - **Simon Frasch** @ CSCS: GPU nuFFT library
  - **Michele Bianco**: scientific validation
  - **Shreyam Krishna:** scientific validation
  - **Arpan Das**: measurement set interface
  - **Mattheiu Simeoni, Paul Hurley, Sepand Kashani:** Algorithm development/expertise

Radio Interferometric Imaging Process

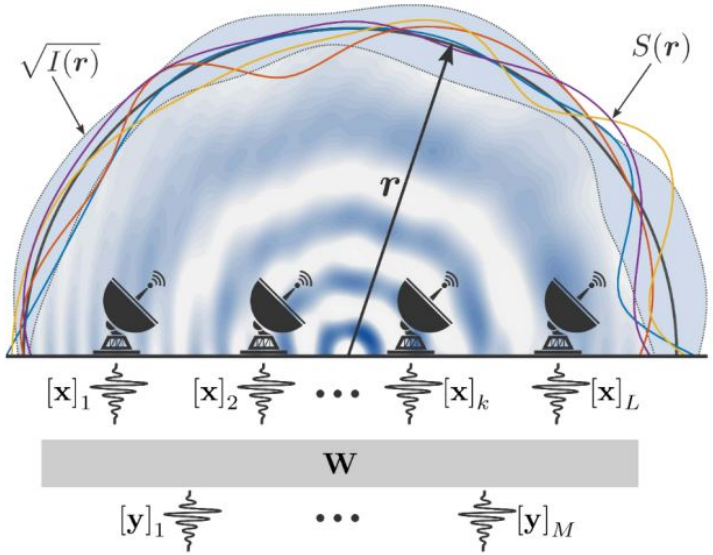

Single Antenna Signal

Visibilities

$$y = \Psi^* S \quad \text{Correlator} \quad y_i y_j = Y$$

Best reconstructed source emissions

$$\hat{I} = \tilde{D}Y = \tilde{\Psi} E[y_i y_j *] \tilde{\Psi}^*$$

Find a least squares fit for the sky image.

Bluebild Algorithm

- Flexible continuous spherical imager for interferometric applications
- Solves for I(r) in $\int_{\mathbb{S}^2} I(r) e^{-j<r,p_i-p_j>} dr = V_{ij}$ by framing a generalised eigenvalue problem and decomposing visibilities into different eigenvectors, via fPCA → $\mathbf{E}[yy^*]\alpha = \sum_{a=0}^{N_{Station}} \lambda_a G_\Psi \alpha_a$
- Eigenvector + sampling operator gives eigenfunctions. These give eigenimages - independent and sorted by energy. Can be truncated (automatic denoising) or filtered.
- 3D NuFFT Type-3
- Low computational complexity and affinity for parallel execution

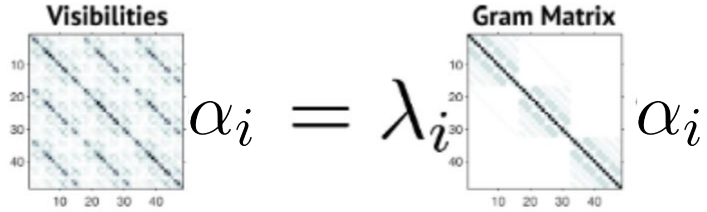

$$\alpha_i = \lambda_i \alpha_i$$

Normalised Eigenfunctions

$$\epsilon_m = \frac{\Psi \alpha_m}{||\Psi \alpha_m||} = \frac{\Psi \alpha_m}{\sqrt{\alpha_m^H G_\psi \alpha_m}}$$

$$\hat{I}(r) = \sum_m \lambda_m |\epsilon_m(r)|^2 = \sum \lambda_m \frac{|\Psi \alpha_m|^2}{v_m^H G_\Psi \alpha_m}$$

Bluebild Imaging Plus Plus (BIPP) Paper

1. arXiv:2310.09200 [pdf, other] astro-ph.IM

BIPP: An efficient HPC implementation of the Bluebild algorithm for radio astronomy

Authors: Emma Tolley, Simon Frasch, Etienne Orliac, Shreyam Krishna, Michele Bianco, Sepand Kashani, Paul Hurley, Matthieu Simeoni, Jean-Paul Kneib

Abstract: ...using the theory of sampling and interpolation operators. We present an HPC implementation of the Bluebild algorithm for radio-interferometric imaging: Bluebild Imaging++ (**BIPP**).... ▽ More

Submitted 13 October, 2023; **originally announced** October 2023.

Comments: 18 pages, 12 figures

- C++ ported version with python wrapper for wider community release
- HPC implementation with support for CUDA (NVIDIA) and HIP (AMD)
- Support for MWA, LOFAR, Oskar SKA-Low measurement sets
- Domain partitioning inbuilt
- No deconvolution - only dirty images
- Github: https://github.com/epfl-radio-astro/bipp
- Arxiv: https://arxiv.org/abs/2310.09200

Standard Synthesis

- For each t, f make image from visibilities using fourier synthesis.
- Stack and average images across t, f
- $O(T F N_{pixel} N_{antenna} N_{eig})$

nuFFT Synthesis

- Collect visibilities across t, f
- Perform nuFFT on collected visibilities
- $O(F N_{eig}((N^2_{antenna} T + N_{pix}) \log(tol)^3 + N_{pix} + N_{mesh}(\log N_{mesh}+1)))$

Where T - time steps, F - frequency channels, $N_{eig} < N_{antenna}$, tol - error tolerance of nuFFT, N_{mesh} - mesh size set by nuFFT based on antenna positions

Inter-solution Consistency

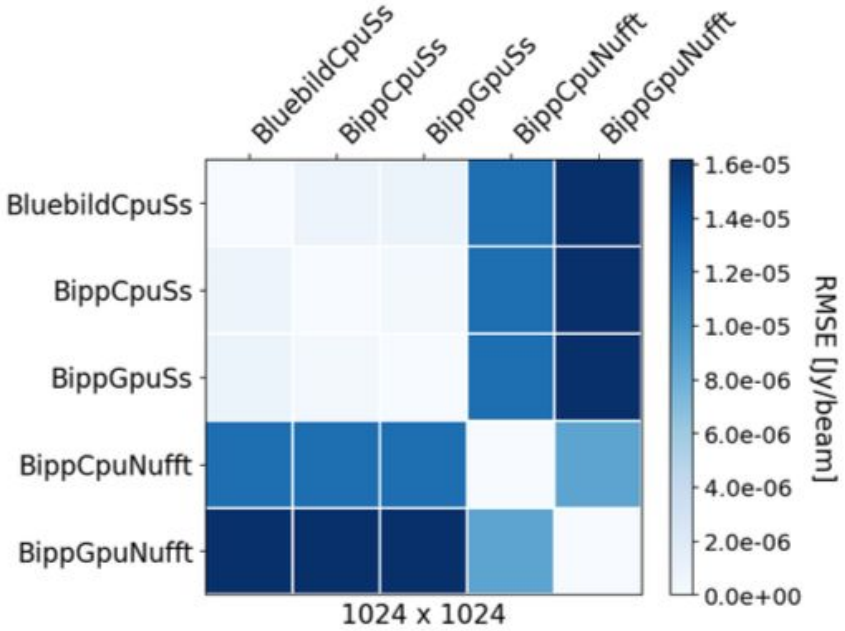

Figure 2. Inter-solution consistency between the different implementations of Bluebild for images of 1024 × 1024 pixels and produced by combining all positive eigenvalues into a single layer. Similar results are obtained when clustering eigenimages into 2, 4 or 8 positive energy levels, see Section 2.4. For completeness, similar plots for image widths of 256, 512 and 2048 pixels are provided in Appendix B1.

Point Source Recovery

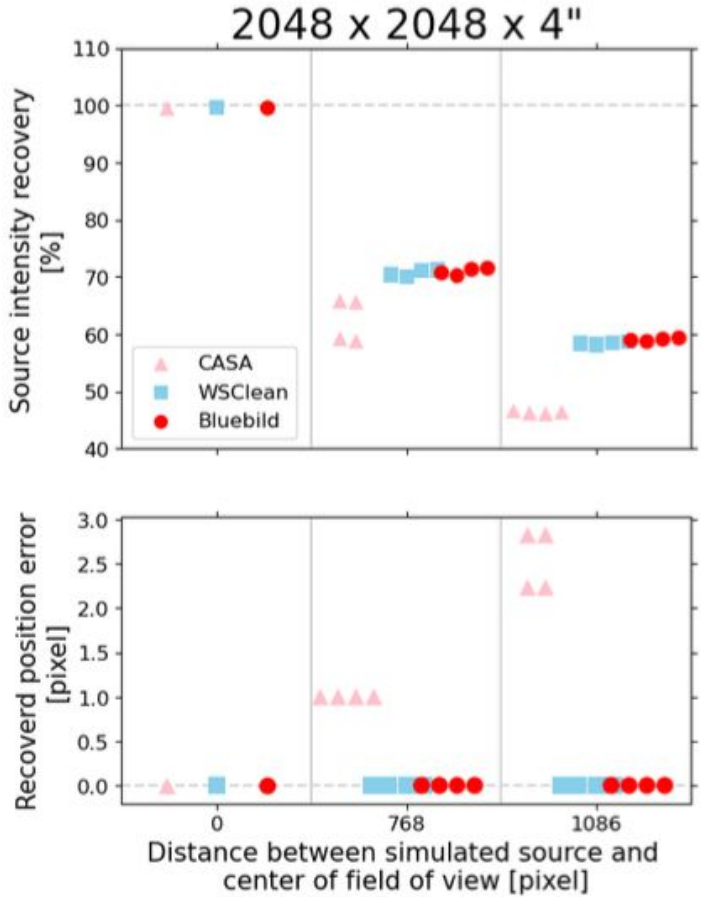

Figure 3. Top plot: recovered intensities given in percentage of the simulated intensity (1 Jy point sources) and bottom plot: distance between the recovered source positions and the simulated ones, in pixels, all plotted against the distance in pixels to the centre of the field of view. A recovery superior to 100% indicates an overestimation of the simulated source, and vice versa. The `BIPP` solution (in red) was obtained with `BIPP` NUFFT GPU (`BippNufftGpu`) implementation for an image of 2048 × 2048 pixels.

9 Point Source Recovery + Residuals

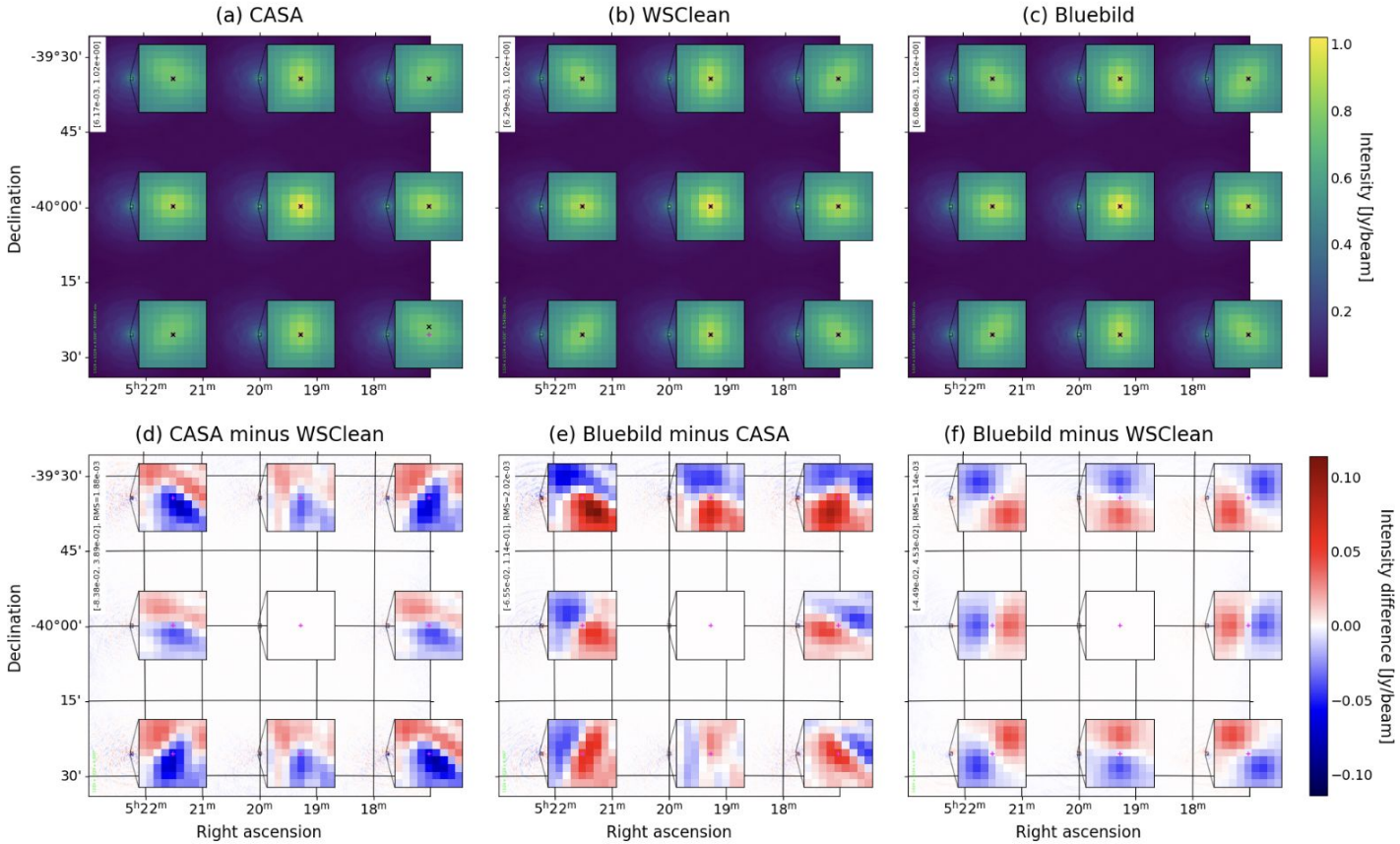

(a) Using BIPP NUFFT Synthesis GPU (`BippNufftGpu`)

Toothbrush cluster Recovery + Residuals

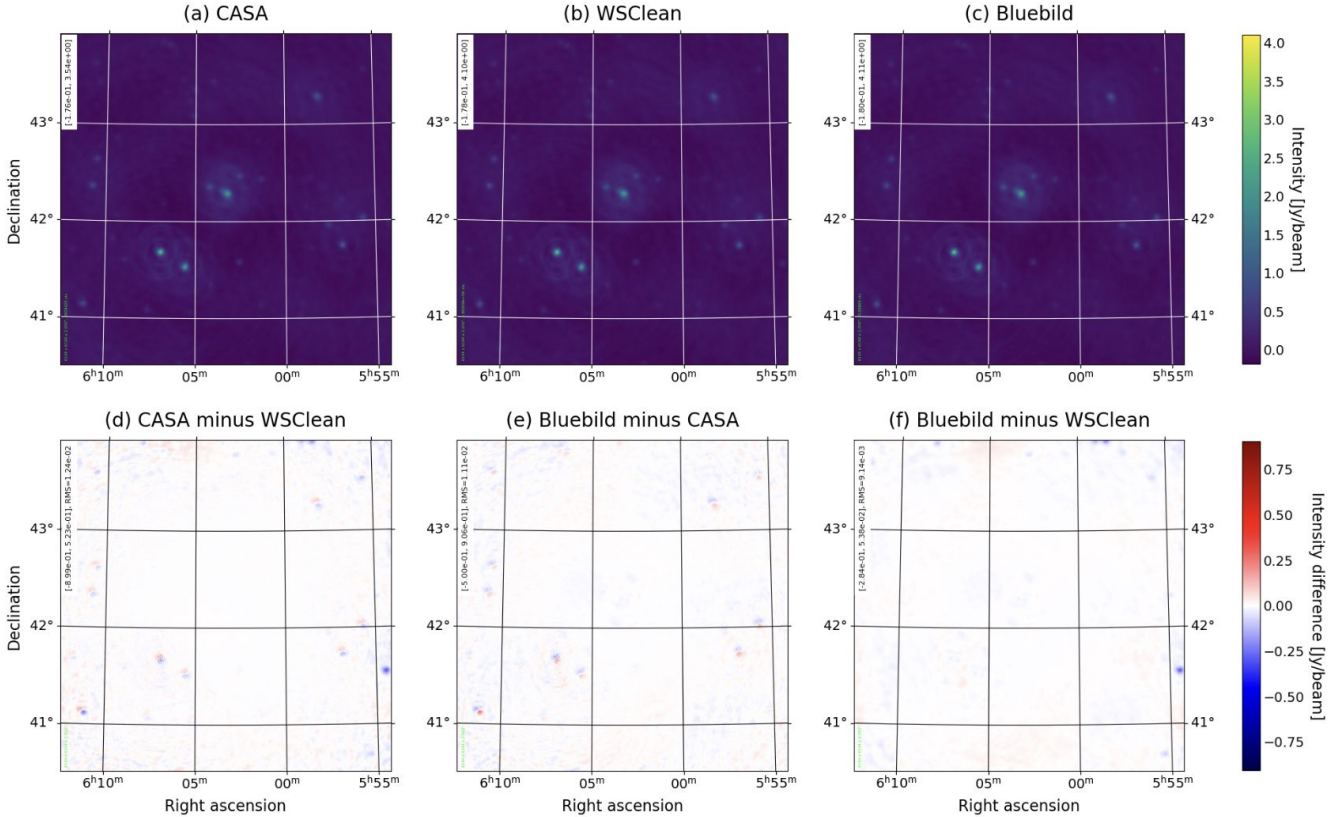

Figure 5. Top row: dirty maps produced with (a) `CASA`, (b) `WSClean`, (c) `BIPP` using real LOFAR data from the Toothbrush cluster RX J0603.3+4214 dataset from Pan et al. (2017). Images produced are 6144 by 6144 pixels of 2" angular resolution. Bottom row: differences between the following pairs of dirty maps: (d) `CASA` minus `WSClean`, (e) `BIPP` minus `CASA` and (f) `BIPP` minus `WSClean`.

Benchmarking

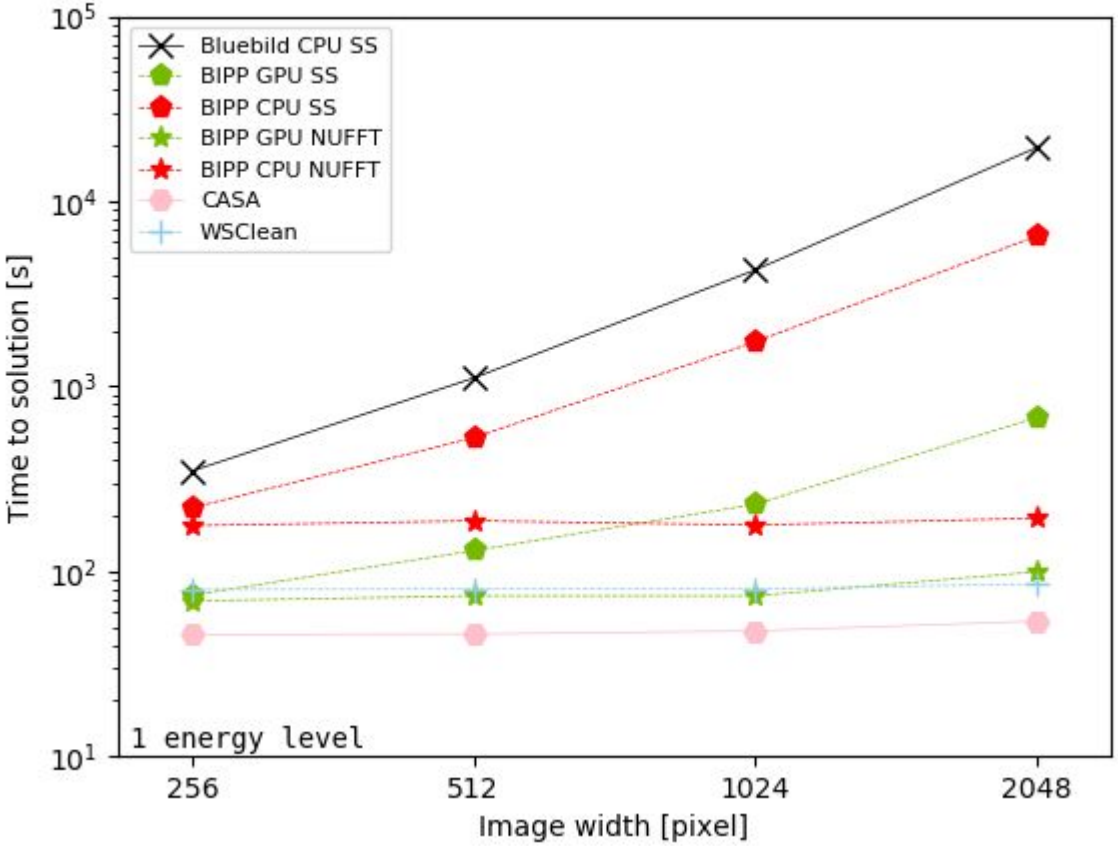

GLEAM catalog point sources

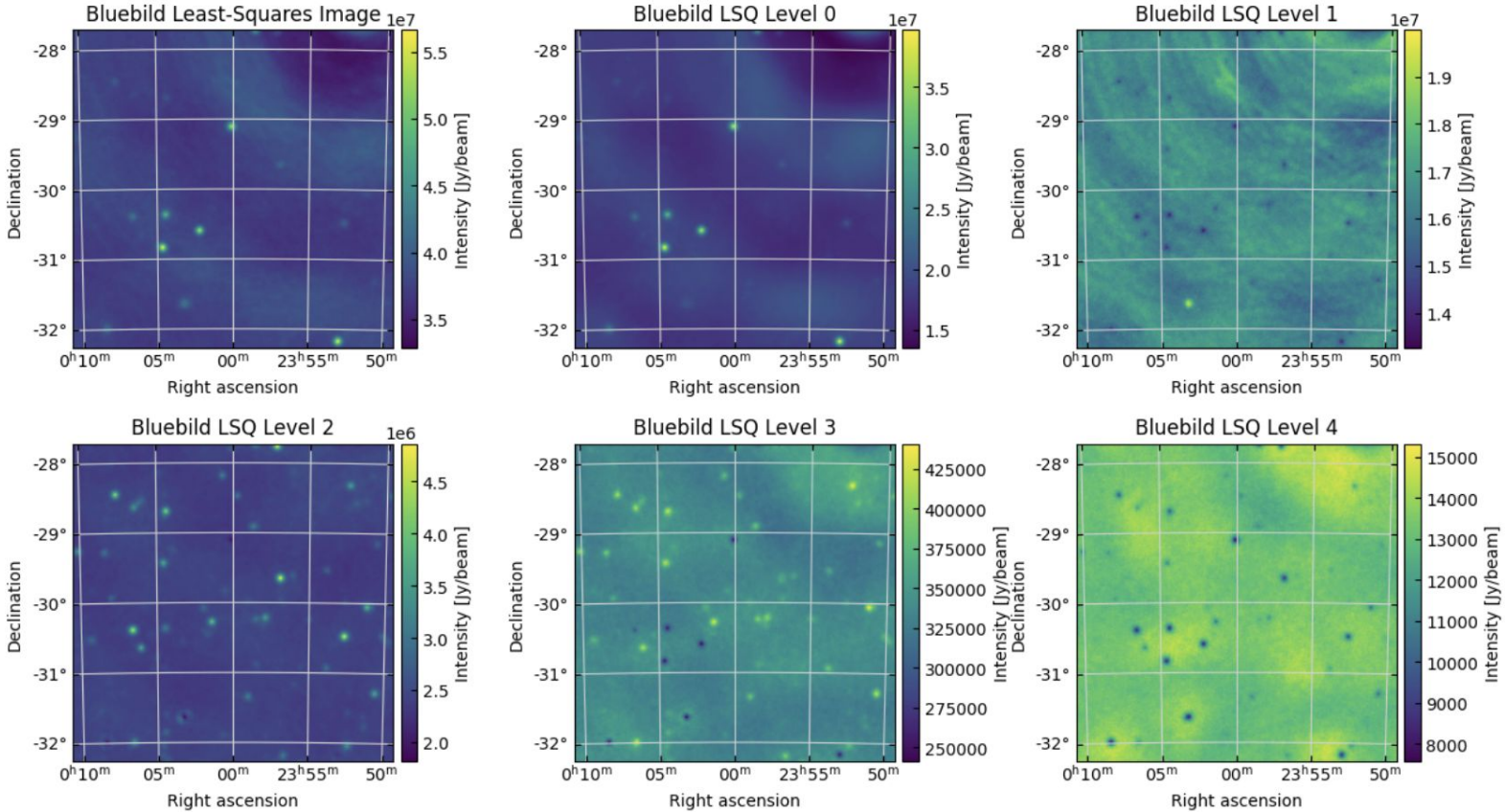

Figure 7. Simulated data of the MWA-GLEAM catalogue and decomposition into four energy levels with BIPP. The top-left Figure shows the LSQ image. The eigenvectors are separated into five energy levels based on their intensity, shown in order of decreasing intensity from left to right, top to bottom.

Losito extended emission

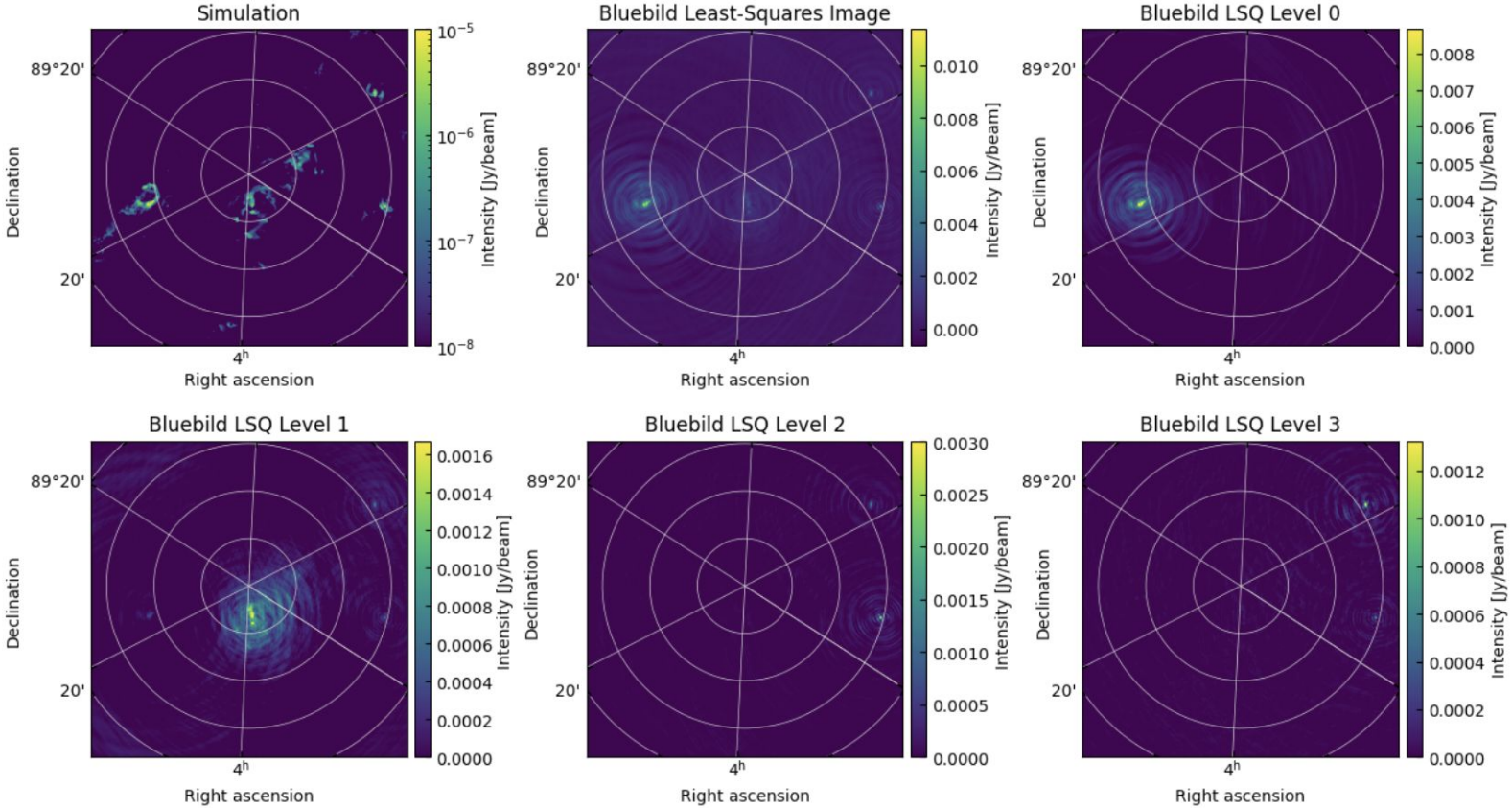

Figure 8. Simulated data with the `LoSiTo` code decomposed into four eigen-levels by `BIPP` functional PCA. The top-left panel shows the sky model employed as input for `LoSiTo`. The top-centre panel shows the least-squared image of the combined eigenimages, equivalent to a dirty image. From left to right, top to bottom, the four eigenimages are separated into five levels based on the k-means algorithm.

Effect of the Gram Matrix

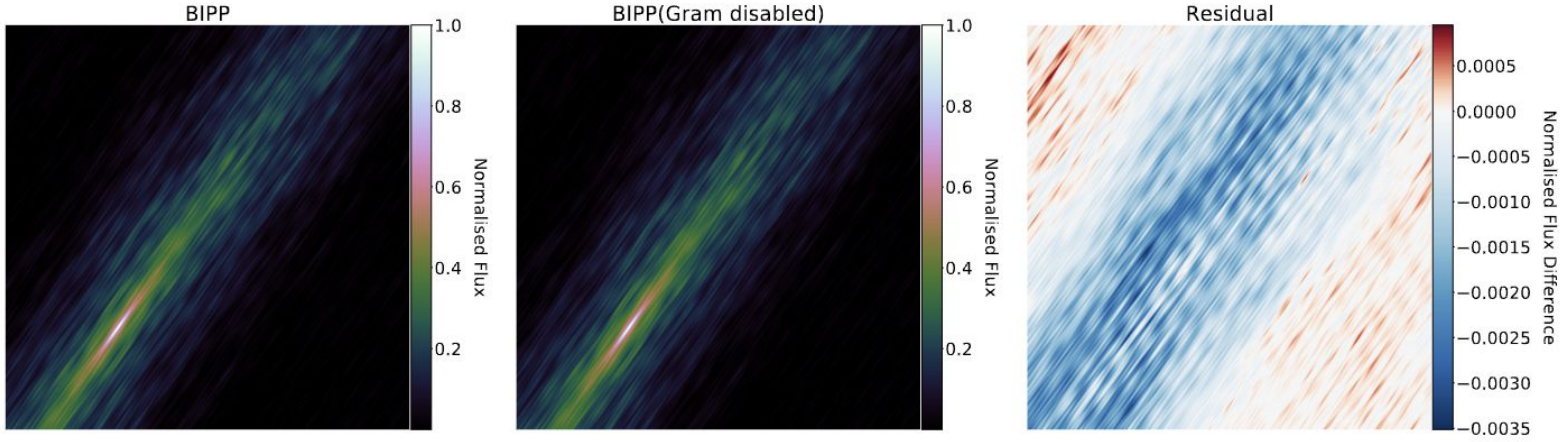

Figure A2. The effect of using the Gram matrix for the generalized eigenvalue decompositon in BIPP reconstructed images at 53MHz. The left column subplot contains the BIPP image normalised by its maximum value. The middle subplot contains the reconstructed BIPP image with the Gram matrix set to identity. This has also been normalised by its maximum value. The right subplot shows the residual obtained when taking the difference between the BIPP images reconstructed with and without the Gram matrix. The presence of negative (blue) features in the residual image tells us that the sidelobes are slightly stronger when the Gram matrix is turned off.

Ongoing and Future Work:

- MPI BIPP
- Visibility weighting
- Faster .ms interface
- Radler (Radio Astronomical Deconvolution Library) and other deconvolution incorporation
- Bluebild point source removal paper (Krishna et al)
- Bluebild algorithm paper (Simeoni et al)

Contact me at shreyam.krishna@epfl.ch for any questions!

BIPP Github:

Contact me at shreyam.krishna@epfl.ch for any questions!

Backup Slides Start Here

CLEAN family of algorithms

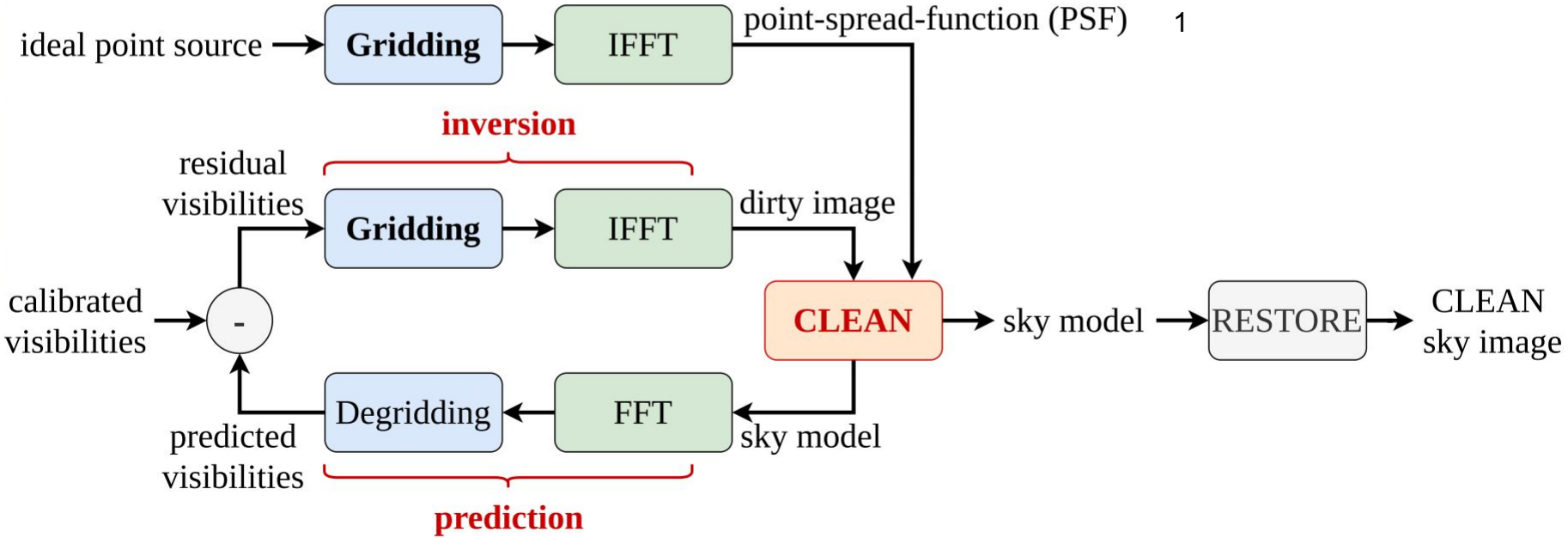

1: [Corda 2022]

Gram Matrix Visualised

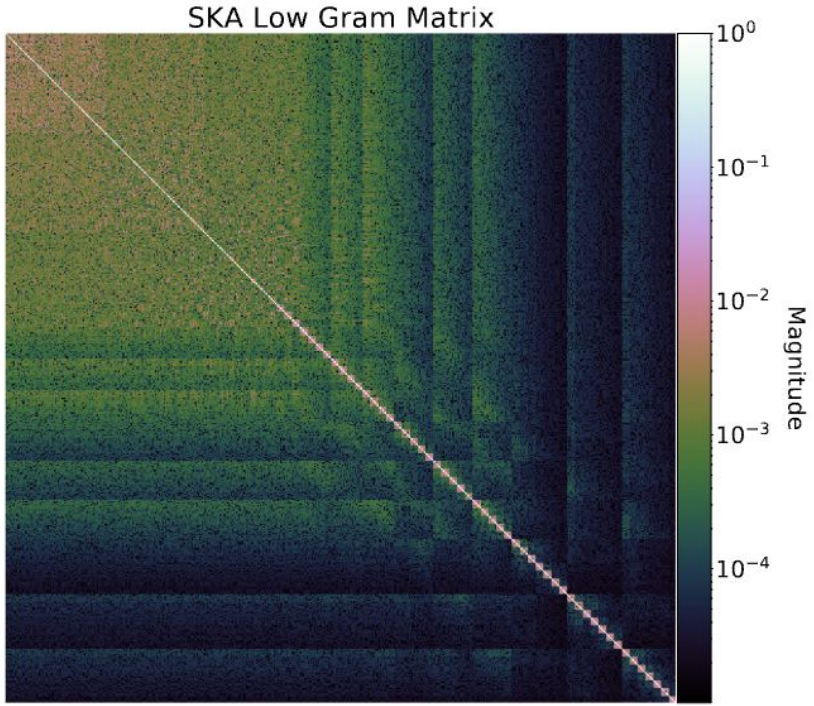

Figure A1. The Gram matrix visualised for the simulated SKA-Low array at 53 MHz.

Inter-solution Consistency (extended)

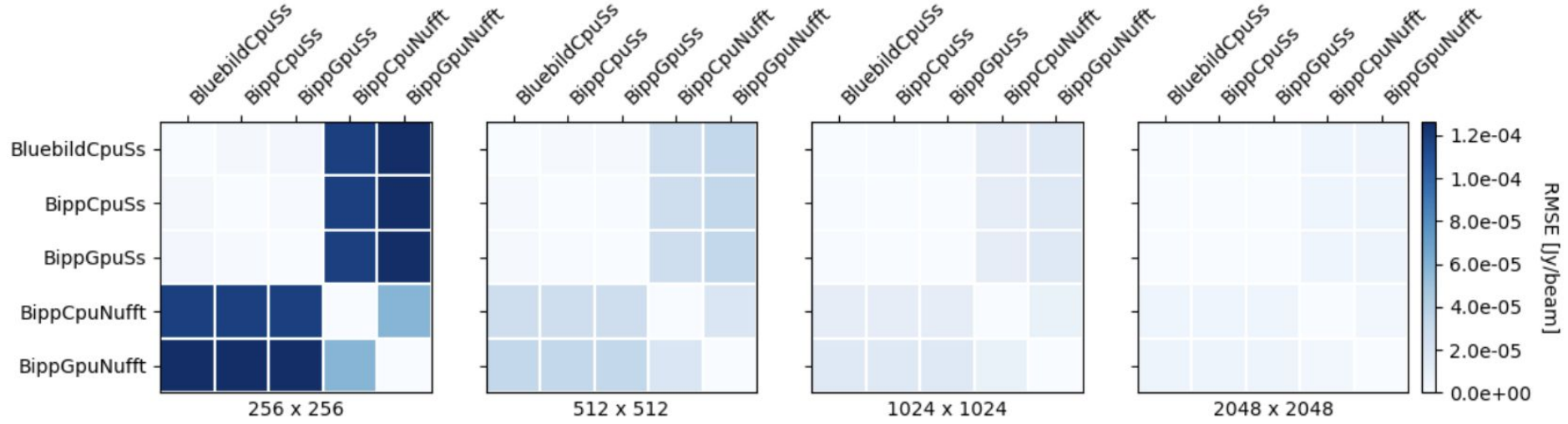

Figure B1. Inter-solution consistency between the different implementations of Bluebild decomposed over image resolution, for images produced considering a single positive energy layer. Similar results are obtained using 2, 4 or 8 positive energy levels.

nuFFT GPU v/s SS CPU

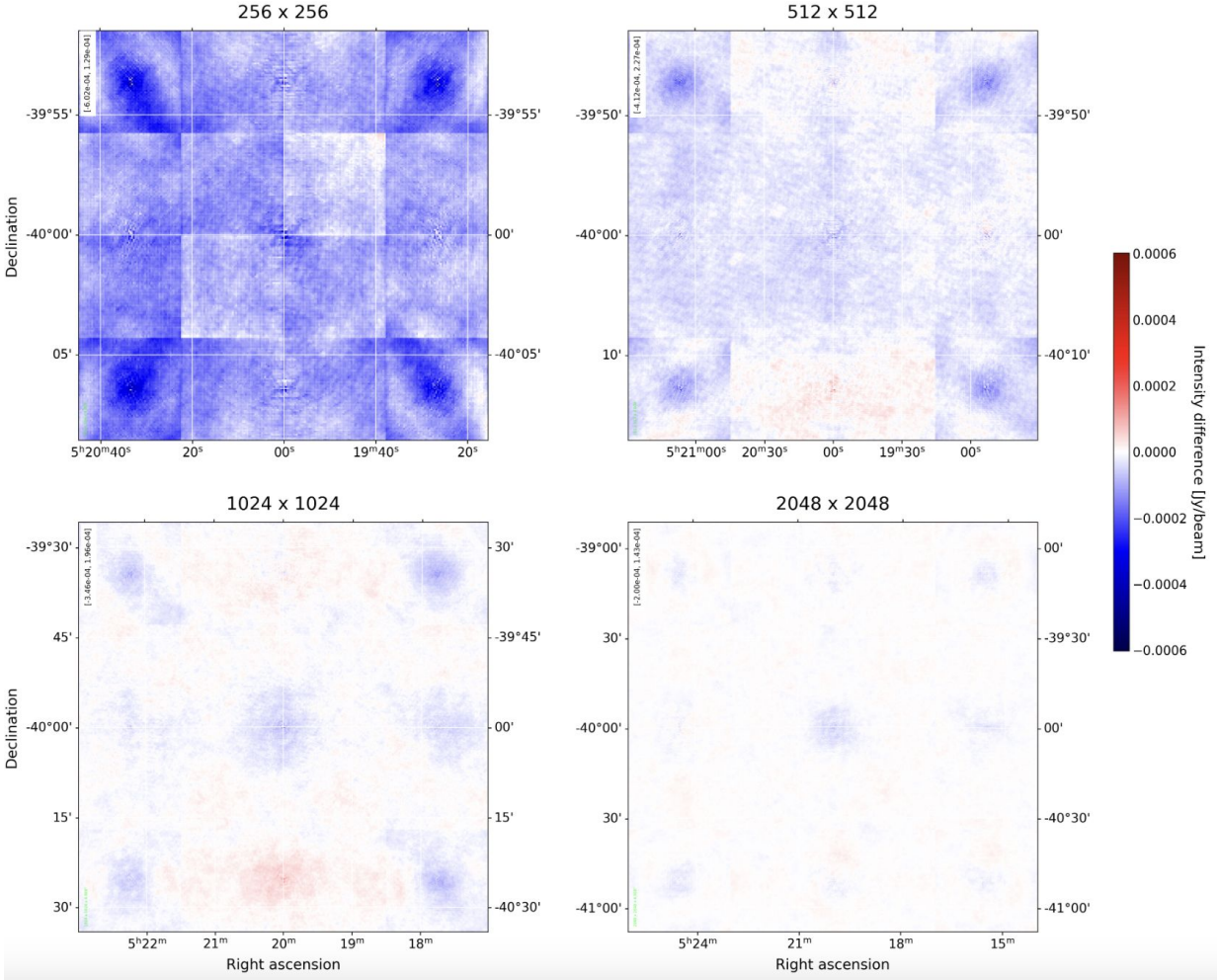

Bluebild Algorithm[1]
Psuedo-Inverse Least Squares Solution

$$\tilde{\Psi} = \Psi G_{\Psi}^{-1} = \Psi\left(\Psi^{*}\Psi\right)^{-1}$$

$$\hat{I}(r) = \tilde{\Psi}\mathbf{E}[yy^{*}]\tilde{\Psi}^{*} = \Psi G_{\Psi}^{-1}\mathbf{E}[yy^{*}]G_{\Psi}^{-1}\Psi^{*}$$

$$\hat{I}(r) = \sum_{m} \lambda_m |\epsilon_m(r)|^2$$

$$\epsilon_m = \Psi\alpha_m \qquad \hat{I}(r)\Psi\alpha_m = \lambda_m\Psi\alpha_m$$

$$\mathbf{E}[yy^{*}]\alpha_m = \lambda_m G_{\Psi}\alpha_m$$

1:[Simeoni, Hurley and Kashani, 2023]